Supporting Information

Ca^{2+} and Ga^{3+} doped $LaMnO_3$ perovskite as highly efficient and stable catalyst for two-step thermochemical water splitting

Lulu Wang,[a] Mohammad Al-Mamun,[a] Yu Lin Zhong,[a] Lixue Jiang,[a] Porun Liu,[a] Yun Wang,[a] Hua Gui Yang[b] and Huijun Zhao*[ac]

[a]Centre for Clean Environment and Energy, Griffith University, Gold Coast Campus, QLD 4222, Australia

[b]Key Laboratory for Ultrafine Materials of Ministry of Education, School of Materials Science and Engineering, East China University of Science and Technology, 130 Meilong Road, Shanghai 200237 China

[c]Centre for Environmental and Energy Nanomaterials, Institute of Solid State Physics, Chinese Academy of Sciences, Hefei 230031, P. R. China

E-mail: h.zhao@griffith.edu.au; Fax: +61 7 5552 8067; Tel: +61 7 5552 8261

I Experimental Section

Perovskites synthesis

All the perovskite oxides were synthesised by a modified Pechini method.[1] . In brief, stoichiometric amounts of metal nitrate precursors were dissolved in deionized water and heated at 70 °C with continuous stirring. Citric acid was then added to the solution with a molar ratio of 1.5:1 with respect to the metal cations. After 10 min, ethylene glycol (ethylene glycol: citric acid molar ratio = 1:1) was added to the mixture and heated at 90 °C until a brownish gel was obtained. The resulting gel was transferred to an electric oven and kept at 120 °C for 12 h to obtain a resin. The resin was then collected and ground with a mortar and pestle. The final perovskite oxide powder was prepared by calcining the resin at 1300 °C for 6 h to remove any remaining organics or nitrates.

Characterisations

The X-ray diffraction (XRD) patterns of the samples were collected with a Bruker D8 X-ray diffractometer operated at 40 kV with the current of 25 mA using a Cu Kα radiation. The measurements of 2θ symmetrical scans were carried out in the range of 20–80 ° with a step size of 0.02 ° and a scanning rate of 2 °/min, respectively. Phase identification was conducted through comparisons with the standard Inorganic Crystal Structure Database (ICSD). Scanning electron microscopy (SEM, JSM- JSM-7100), energy dispersive X-ray (EDX, JSM-7100) mapping and transmission electron microscope (TEM, Tecnai F20) techniques were also employed to characterise the surface morphology and elemental distribution within the samples.

Thermochemical H_2O splitting test

The two-step thermochemical H_2O splitting activity was investigated using a laboratory-scale fix-bed reactor, as shown in Fig. S4. To facilitate effective testing, the freshly-prepared perovskite samples (~ 0.5 g) were transferred into a solid porous monolith structure by mixing with isopropanol then fired at 1300 °C for 6 h in air.[2] The prepared redox sample was then packed at the centre of an alumina tubular reactor coupled within a high temperature programmable electric furnace (MTI, KSL-1800X-S60). Ar (ultra-high purity ~ 99.99%) was used as a carrier gas and the flow rate was controlled by a mass flow controller (Alicat Scientific). The thermal reduction step was carried out by heating the perovskite sample to 1300 °C and holding for 1 h under an Ar flow rate of 200 sccm (the oxygen partial pressure was ~20 ppm). The temperature was then allowed to decrease to 900 °C for H_2O splitting. The

temperature increase and decrease rates were fixed at 10 °C/min. The water was introduced into the chamber by a water pump (Easypump, BT100N), then vaporised and mixed with Ar gas (the volume ratio of vapour in the mixture gas was ~ 40%). The whole H_2O splitting process was maintained for 1 h to complete the re-oxidation process. During the thermal reduction and H_2O splitting processes, the O_2 and H_2 produced were detected by mass spectrometer (MS, Omni Star GSD 320). For quantitative measurement of evolved gas, the ion current signal of the MS result was calibrated by standard O_2 and H_2 gases.

The re-oxidation yield (α) of thermochemical H_2O splititng test was calculated as follow,

$$\alpha = (n_{H_2} / 2n_{O_2}) \times 100\%$$

where n_{O_2} and n_{H_2} repersent the total amount (mole weight) of O_2 and H_2 evolved during two-step thermochemical H_2O splitting process.

II Supporting Figures

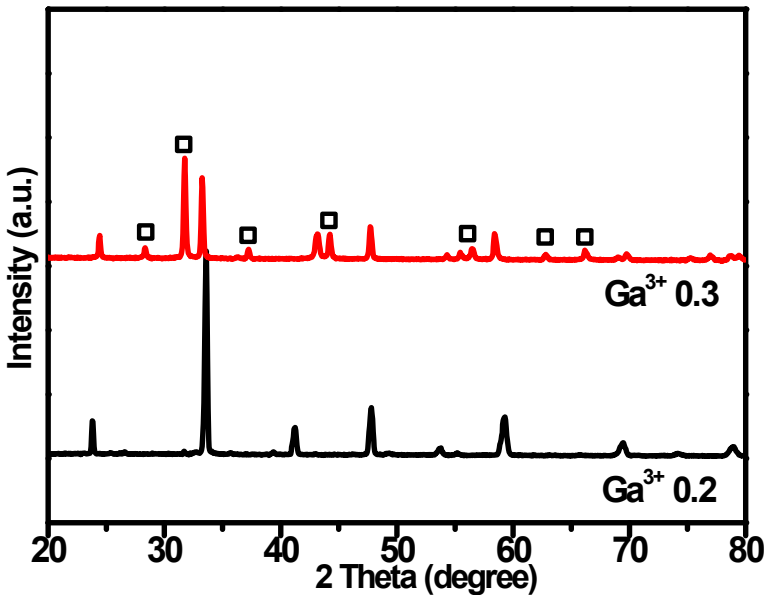

Fig. S1 XRD patterns of $LaMnO_3$ based perovskites with the Ga^{3+} doping content of 0.2 (black) and red (0.3) on the B site. The square represents the impurity of Ga_2O_3 in the fabricated perovskite sample.

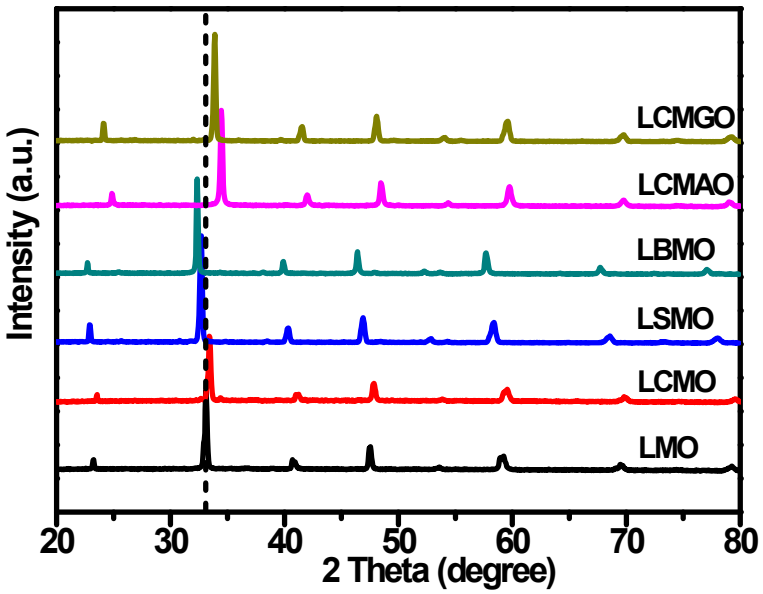

Fig. S2 XRD patterns of parent $LaMnO_3$ and A site (Ca^{2+}, Sr^{2+}, Ba^{2+}) and B site (Al^{3+} and Ga^{3+}) doped $LaMnO_3$ perovskites.

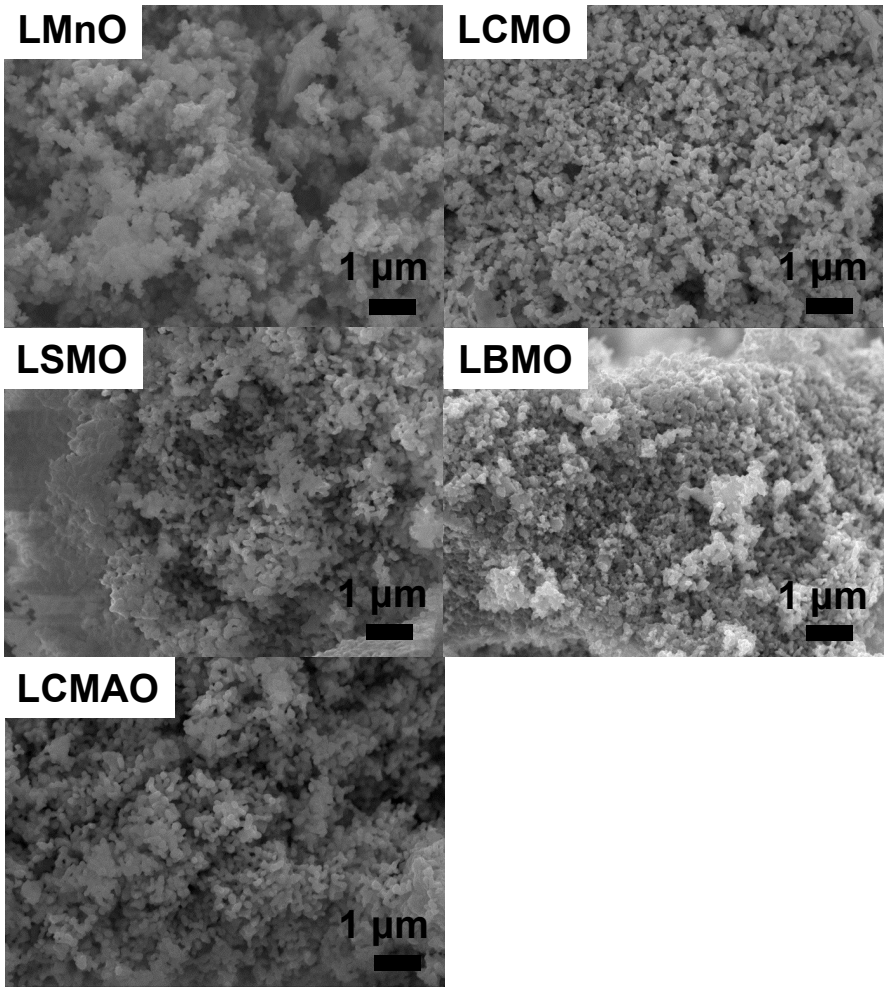

Fig. S3 SEM images of of parent $LaMnO_3$ and A site (Ca^{2+}, Sr^{2+}, Ba^{2+}) and B site (Al^{3+} and Ga^{3+}) doped $LaMnO_3$ perovskites..

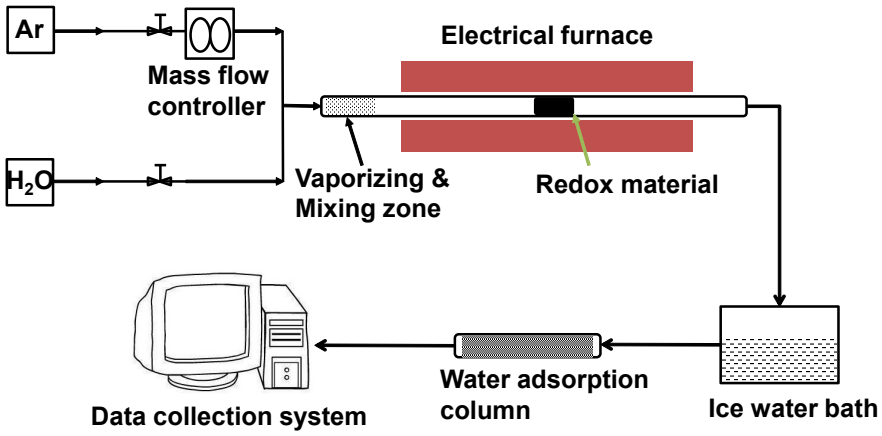

Fig. S4 Two-step thermochemical H_2O splitting set-up for H_2 production.

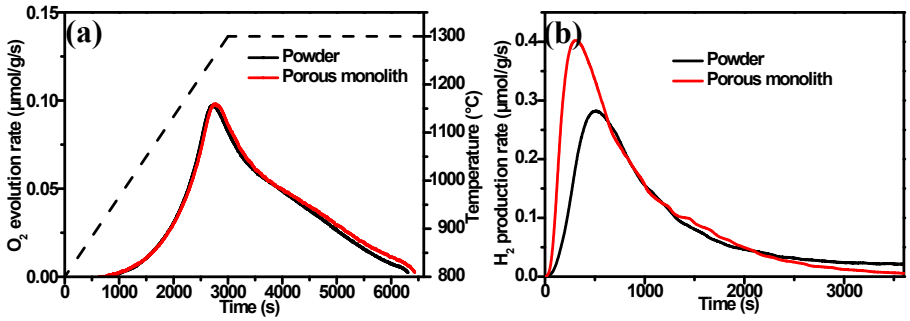

Fig. S5 A comparison of O_2 evolution and H_2 production between perovskite powder and porous monolith during two-step thermochemical H_2O splitting process.

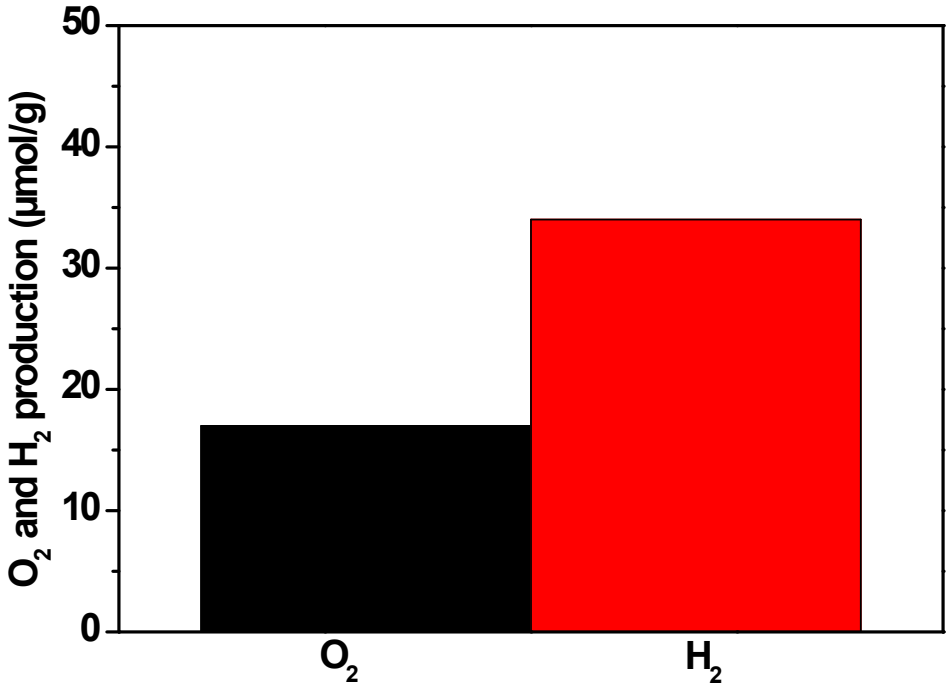

Fig.S6 O_2 and H_2 production results of CeO_2 from thermochemcial H_2O splitting operated between 1300 and 900 °C.

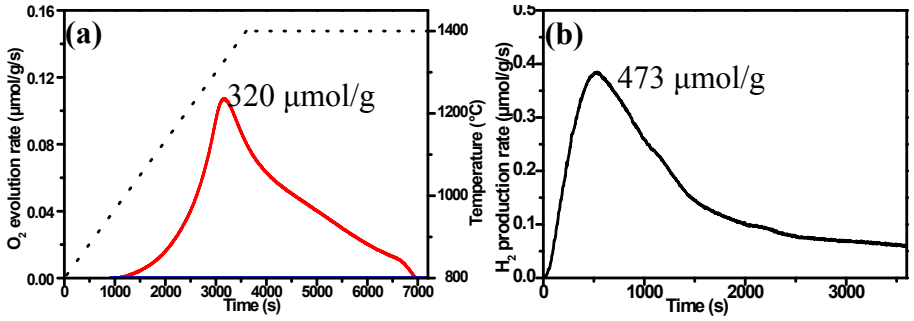

Fig. S7 (a) O_2 evolution and (b) H_2 production curves of $La_{0.6}Ca_{0.4}Mn_{0.8}Ga_{0.2}O_3$ perovskite oxide with the two-step thermochemical H_2O splitting carried out between 1400 and 900 °C.

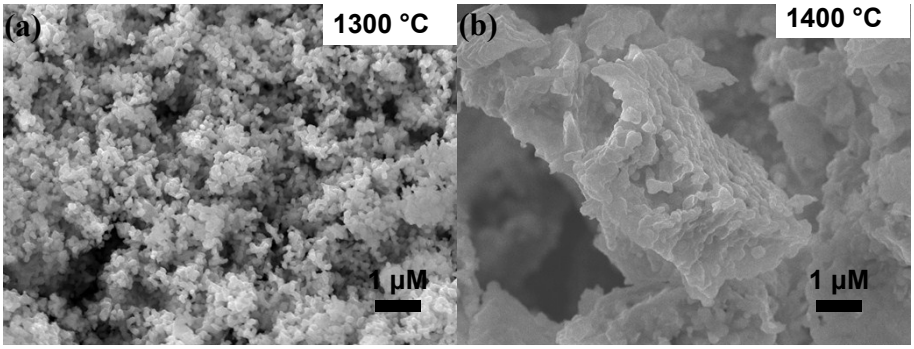

Fig. S8 SEM images of $La_{0.6}Ca_{0.4}Mn_{0.8}Ga_{0.2}O_3$ perovskite oxide after thermally reduced at (a) 1300 °C and (b) 1400 °C.

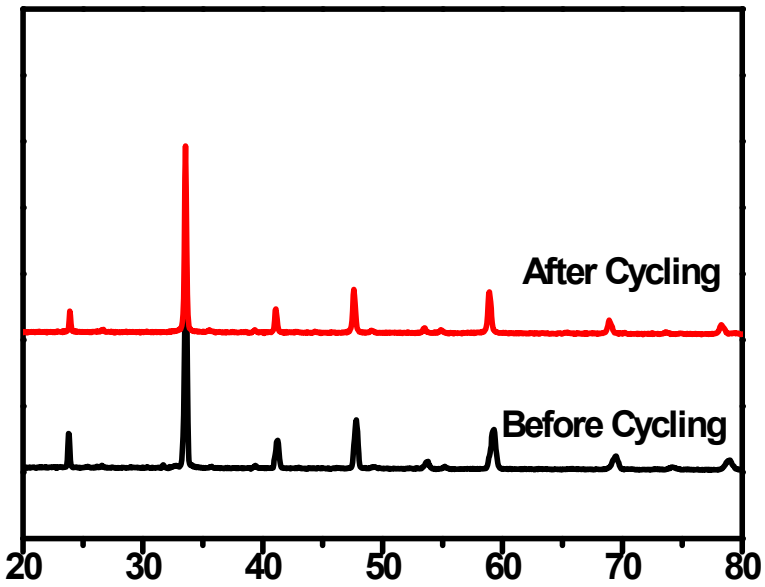

Fig. S9 XRD patterns of LCMGO before (black) and after (red) the thermochemical cycling measurements

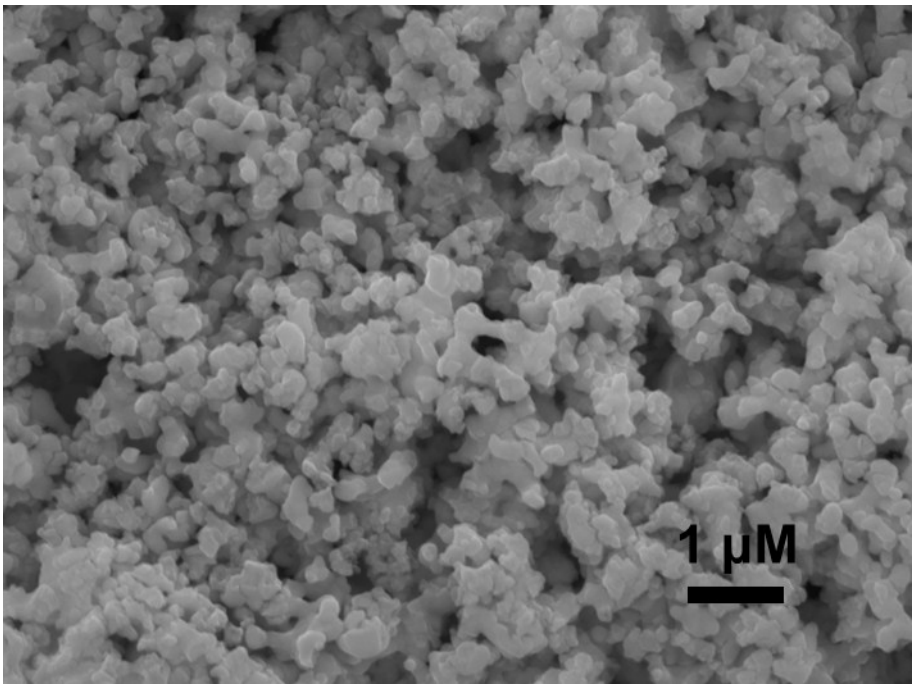

Fig. S10 SEM image of LCMGO after the two-step thermochemical H_2O splitting cycling test operated between 1300 and 900 °C.

Table S1 BET surface area of $LaMnO_3$ based perovskites with various metal ions doped before and after two-step thermochemical H_2O splitting process.

Perovskite sample	BET surface area before thermochemical test (m^2/g)	BET surface area after thermochemical test (m^2/g)
$La_{0.6}Ba_{0.4}MnO_3$	10.4	7.9
$La_{0.6}Sr_{0.4}MnO_3$	11.5	9.4
$La_{0.6}Ca_{0.4}MnO_3$	14.2	11.5
$La_{0.6}Ca_{0.4}Mn_{0.8}Al_{0.2}O_3$	16.9	13.4
$La_{0.6}Ca_{0.4}Mn_{0.8}Ga_{0.2}O_3$	19.6	15.2

Table S2 Comparison of thermochemical performances of the present study with those reported by other perovskite type catalyst and benchmark CeO_2 in the literature.

Redox Catalyst	Thermal reduction temperature (°C)	O_2 evolution (μmol/g)	H_2 production (μmol/g)	Re-oxidation yield (%)	Ref.
$Ba_{0.5}Sr_{0.5}Co_{0.8}Fe_{0.2}O_3$	1000	600	83	7	3
$La_{0.6}Sr_{0.4}Cr_{0.8}Co_{0.2}O_3$	1200	154	50	16	4
$La_{0.5}Sr_{0.5}Co_{0.8}Fe_{0.2}O_3$	1200	503	90	9	3
$La_{0.6}Ca_{0.4}Mn_{0.8}Ga_{0.2}O_3$	1300	212	401	95	This study
$LaSrCoO_4$	1300	268	161	30	3
$La_{0.6}Sr_{0.4}Mn_{0.4}Al_{0.6}O_3$	1350	120	220	92	5
$La_{0.5}Sr_{0.5}Mn_{0.95}Sc_{0.05}O_3$	1400	390	250	32	6
$La_{0.6}Sr_{0.4}MnO_3$	1400	219	397	91	7
$La_{0.5}Sr_{0.5}MnO_3$	1400	298	195	33	3
$La_{0.6}Ca_{0.4}MnO_3$	1400	272	407	75	8
$Y_{0.5}Sr_{0.5}MnO_3$	1400	481	320	33	9
$Y_{0.5}Ca_{0.5}MnO_3$	1400	593	310	26	9
CeO_2	1400	66	144	109	10
CeO_2	1640	111	178	80	11

Supporting References

1. Y.-S. Han and H.-G. Kim, *J. Power Sources*, 2000, **88**, 161.
2. Y. Hao, C. K. Yang and S. M. Haile, *Chem. Mater.*, 2014, **26**, 6073.
3. A. Demont, S. Abanades and E. Beche, *J. Phys. Chem. C*, 2014, **118**, 12682.
4. A. H. Bork, M. Kubicek, M. Struzik and J. L. M. Rupp, *J. Mater. Chem. A* 2015, **3**, 15546.
5. A. H. McDaniel, E. C. Miller, D. Arifin, A. Ambrosini, E. N. Coker, R. O'Hayre, W. C. Chueh and J. H. Tong, *Energy Environ. Sci.*, 2013, **6**, 2424.
6. S. Dey, B. S. Naidu and C. N. R. Rao, *Dalton Trans.*, 2016, **45**, 2430.
7. C. K. Yang, Y. Yamazaki, A. Aydin and S. M. Haile, *J. Mater. Chem. A*, 2014, **2**, 13612.
8. S. Dey, B. S. Naidu, A. Govindaraj and C. N. R. Rao, *Phys. Chem. Chem. Phys.*, 2015, **17**, 122.
9. S. Dey, B. S. Naidu and C. N. R. Rao, *Chem. Eur. J.*, 2015, **21**, 7077.
10. A. Le Gal, S. Abanades and G. Flamant, 2011, **25**.
11. W. C. Chueh, C. Falter, M. Abbott, D. Scipio, P. Furler, S. M. Haile and A. Steinfeld, *Science*, 2010, **330**, 1797.